

FURTHER PROGRESS ON NONDESTRUCTIVE DIAGNOSIS OF HYBRID MICROELECTRONIC
COMPONENTS USING TRANSMISSION ACOUSTIC MICROSCOPY

J. K. Wang, C. C. Lee, and C. S. Tsai
Center for the Joining of Materials
and
Department of Electrical Engineering
Carnegie-Mellon University
Pittsburgh, PA 15213

ABSTRACT

Recent progress on diagnosis and characterization of defects in hybrid microelectronic components using a transmission scanning acoustic microscope (SAM) operating at 150 MHz is summarized. A simple method has been established to locate (in three dimensions) and classify the defects. The study also shows that two optically identical thick-film resistors having a ratio of 5×10^3 in resistance value exhibit a 43 db contrast in acoustic amplitude.

INTRODUCTION

The characteristics of microelectronic components are greatly affected by the elastic faults or defects such as inclusions, voids, delaminations, and nonuniform particle distribution. Due to impedance mismatch, scattering and absorption associated with a defect, significant attenuation is expected in the transmitted acoustic signal. Therefore, the degree of darkness at an image area is a measure of the acoustic opacity, and thus the irregularity or defect at a corresponding area in the specimen. We had earlier employed a transmission-type scanning acoustic microscope⁽¹⁾ (see Fig. 1), operating at 150 MHz, to image the internal structures of some hybrid microelectronic components.^(2,3)

It is highly desirable to distinguish between a VOID-type defect and an INCLUSION-type defect through quantitative measurement. We have recently found that a definitive distinction can be made by translating the specimen along the lens axis at small increments and recording the corresponding amplitudes and phases of the transmitted signal through the particular defect. The amplitude and phase data obtained indicate not only the depth, size, but also the type of the defect. Phase information is important because the variation in the local acoustic phase is a measure of the acoustic velocity of an isolated defect and also of the interface profile of a mechanical or metallurgical bond.⁽⁴⁾

CAPABILITIES OF THE SCANNING ACOUSTIC MICROSCOPE

The modes of operation and the key parameters of the scanning acoustic microscope (SAM) employed in this study are listed as follows:

Modes of operation:

Transmission Mode	Amplitude
	Phase
	Confocal
	Nonconfocal

Acoustic lenses: $f/4$ (focal length in water = 4 mm)

Spatial resolution: 30 μm in water at 150 MHz
(confocal)

Field of view for the sample: 3×4 (mm^2)

Magnification of acoustic images = 35

Total electrical throughput loss (without specimen):
55 db

Dynamic range: 50 to 70 db at 20 dbm input electrical power, depending on the specimen.

DIAGNOSIS AND CHARACTERIZATION OF HYBRID
MICROELECTRONIC COMPONENTS

The findings on three types of hybrid microelectronic components are now discussed:

Thin-Film Circuits - Defects which result from contaminants and blisters introduced during the fabrication process greatly affect the resistance, adhesion, and solderability of the thin-film circuits. Figures 2(a), (c) show the acoustic micrograph and the amplitude profile of a thin-film resistor (Fig. 2(b) for its cross-sectional view). The defects and the nonuniformity of the multilayer structure are clearly seen. Figure 2(c) shows a differential amplitude variation as large as 30 db.

Thick-Film Circuits - The dark and gray areas in the optical micrographs (Fig. 3(b)) correspond, respectively, to the three individual resistors (100 Ω , 1.3 k Ω , and 500 k Ω) and the conductors of a production-line thick-film circuit (Fig. 3(a)). The acoustic micrographs (Fig. 3(c)) show a high degree of contrast as a function of resistance values. Specifically, a differential attenuation of 43 db is observed between the 100 Ω and the 500 k Ω resistors. Some defects in the form of inclusions are also observable in the resistor and circuit-free regions.

Multilayer Chip Capacitors - The defects referred to in the Introduction are potential causes for a leaky capacitor, and end metallization of poor quality is often a sufficient cause for open-circuit failure.⁽⁵⁾ Figure 4(a) is an example of a faulty end metallization (dark stripes designated as L) in a production-line ceramic chip capacitor (Fig. 4(b)). Figure 5(a) is another capacitor which shows two areas of delamination together with some voids (see Fig. 5(b) for its optical image).

A definitive identification of the above defects was facilitated by comparing the detected signal levels with the noise level. Since the detected signals were buried in noise, the defects should be of the "void"-type. For an "inclusion"-type defect, however, the detected signal level was found to be substantially above the noise level.

The last example, also involving a production-line chip capacitor, serves to demonstrate that the SAM is capable of determining not only defect location (in three dimension) but also defect type. Figures 6(a) to 6(c) show a series of acoustic micrographs obtained for the capacitor shown in Figure 7. Figure 8(a) indicates that area (2.2) is defect-free. However, for area (1.1), there is an "inclusion"-type defect at the depth designated by P since the minimum detected signal (-54 dbm) is well above the noise level. Figure 8(b) shows two "void"-type defects located at different depths A and B since the detected signals are at the same level as noise.

CONCLUSION

We conclude that the transmission SAM operating at several hundred megahertz range is a highly useful technique for nondestructive diagnosis and characterization of thick hybrid microelectronic components.

ACKNOWLEDGEMENTS

Support from the Materials Research Laboratory Section, Division of Materials Research, National Science Foundation under Grant No. DMR72-03297-A03 is gratefully acknowledged.

REFERENCES

1. R. A. Lemons and C. F. Quate, "Acoustic Microscope - Scanning Version," Appl. Phys. Lett., 24, 163 (February 1974).
2. C. S. Tsai, J. K. Wang and C. C. Lee, "Imaging and Characterization of Thick Production-Line Microelectronic Components Using Transmission Acoustic Microscopy," Proceedings of the ARPA/AFML Review of Progress in Quantitative NDE, Report AFML-TR-78-205, Jan. 1979, pp. 257-262.
3. J. K. Wang, C. C. Lee, and C. S. Tsai, "Non-destructive Diagnosis of Thick Production-Line Microelectronic Components Using Transmission Acoustic Microscope," 1978 International Electron Devices Meeting, Technical Digest, pp. 449-451, IEEE Cat. No. 78CH1324-3ED.
4. S. K. Wang, C. C. Lee and C. S. Tsai, "Non-destructive Visualization and Characterization of Material Joints Using a Scanning Acoustic Microscope," 1977 Ultrasonic Symposium Proceedings, pp. 171-175, IEEE Cat. No. 77CH1264-ISU; C. C. Lee, J. K. Wang, S. K. Wang, P. Hower and C. S. Tsai, "Detection and Characterization of Alloy Spikes in Power Transistors Using Transmission Acoustic Microscopy," to appear in the Proceedings of First International Symposium on Ultrasonic Materials Characterization, National Bureau of Standards, Maryland, June 7-9, 1978.

5. T. F. Brennan, "Ceramic Capacitor Insulation Resistance Failures Accelerated by Low Voltage," IEEE Trans. on Electron Devices, ED-26, pp. 102-108, January 1979.

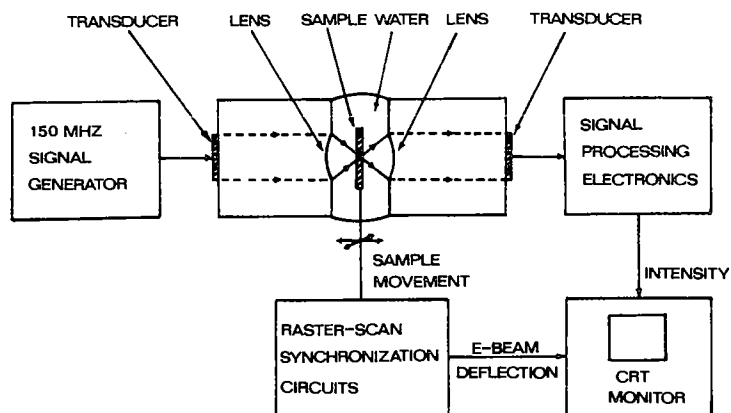
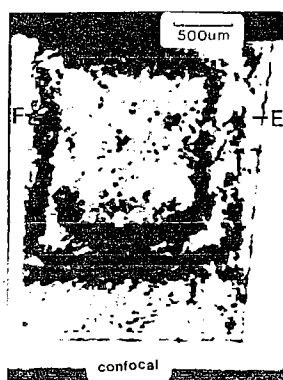
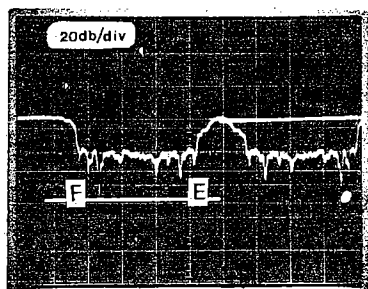


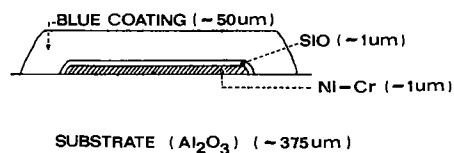
FIG.1
BLOCK DIAGRAM OF A TRANSMISSION SCANNING ACOUSTIC MICROSCOPE



(a)



(c)



(b)

Fig. 2 Imaging of a Thin-Film Chip Resistor

- (a) Acoustic Micrograph
- (b) Cross-Sectional Sketch of the Multilayer Structure
- (c) Acoustic Amplitude Variation Along Line EF

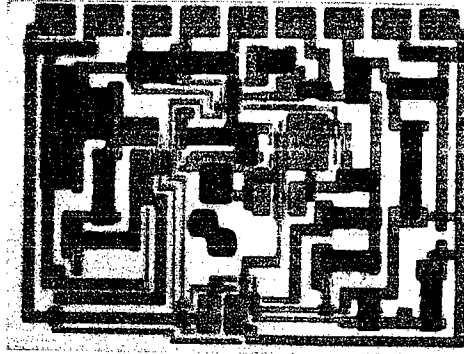


Fig. 3(a) Optical Micrograph of the Production-Line Thick Film Circuit (Thickness: 30 mils) (3.2 X)

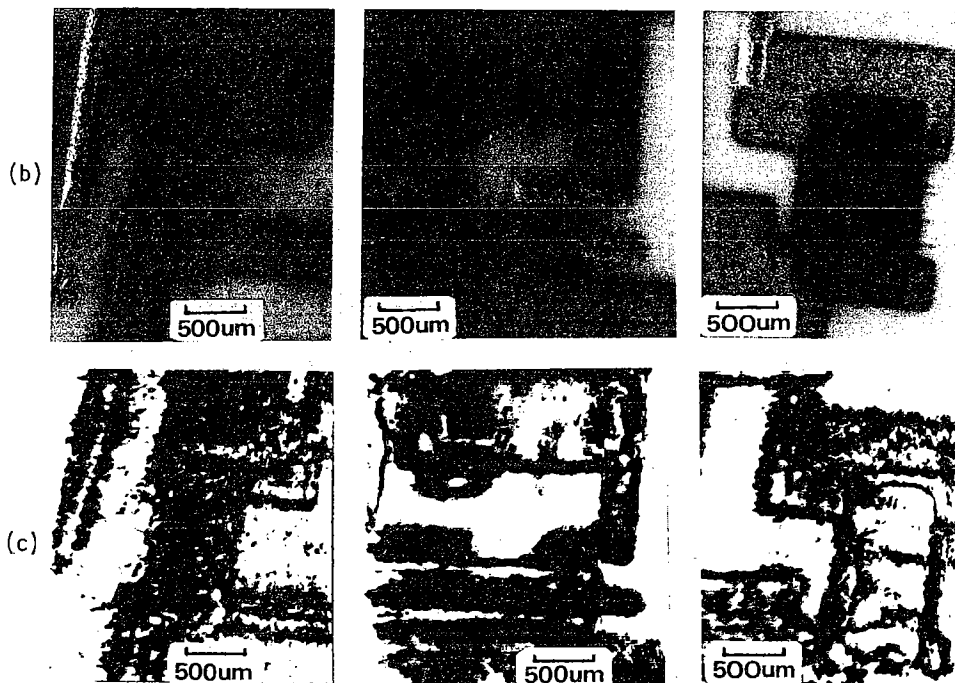


Fig.3(b) Optical Micrographs for Three Resistors (100 Ω , 1.3 K Ω , and 500 K Ω From Left to Right)

3(c) The Corresponding Acoustic Micrographs Depicting High Degree of Contrast



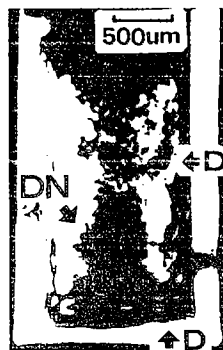
(a)



(b)

Fig. 4(a) Acoustic Micrograph of a Chip Capacitor Showing the Faulty End Metalizations in the Form of Stripes Designated by L

4(b) Optical Micrograph



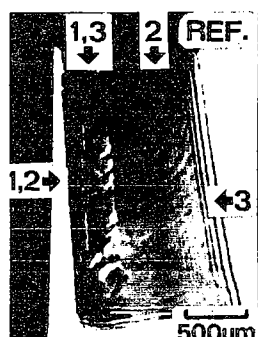
(a)



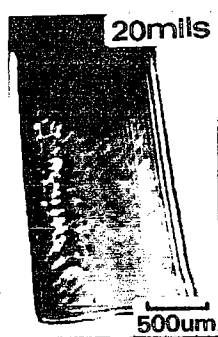
(b)

Fig. 5(a) Acoustic Micrograph of Part of a Chip Capacitor Showing One of the Areas of Delamination Designated by DN, and Voids by D

5(b) Optical Micrograph Showing the Particular Cross Section Where Two Areas of Delamination are Located (Local Brighter Areas)



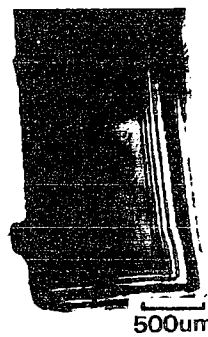
(a)



(b)



(c)



(d)

Fig. 6 Acoustic Micrographs of a Production-Line Chip Capacitor (Thickness: 27 mils)

(b) and (c) Obtained by Displacing the Capacitor Along the Lens Axis by 20 and 40 mils, Respectively, From the Capacitor Position of (a)

(d) Obtained After the Capacitor was Heated at 100°C for 80 Minutes

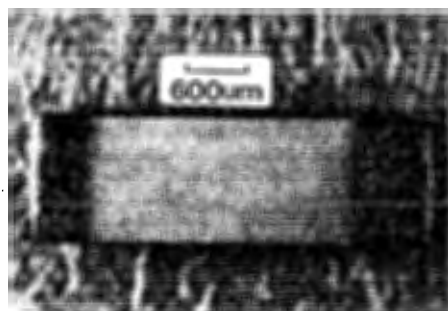


Fig. 7 Photograph of a Production-Line Chip Capacitor (Thickness: 27 mils)

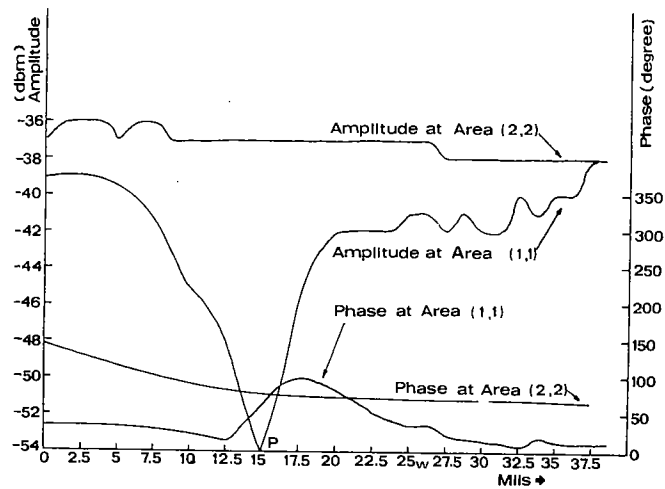


Fig. 8(a) Measured Amplitude and Phase of Transmitted Acoustic Signals as the Chip Capacitor was Translated Along the Lens Axis - An "Inclusion" is Shown to Exist in Area (1,1) at Depth P

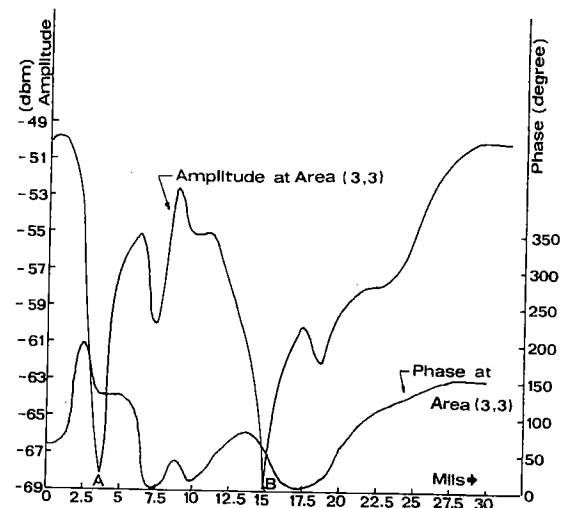


Fig. 8(b) Amplitude and Phase of Transmitted Acoustic Signal (Measured at a Fixed Position of the Chip Capacitor) as the Capacitor was Translated Along the Lens Axis - "Voids" are Shown to Exist at Depths A and B